AIP | Applied Physics Letters

Tailoring palladium nanocontacts by electromigration

Libe Arzubiaga, Federico Golmar, Roger Llopis, Fèlix Casanova, and Luis E. Hueso

Citation: Appl. Phys. Lett. **102**, 193103 (2013); doi: 10.1063/1.4804559
View online: http://dx.doi.org/10.1063/1.4804559
View Table of Contents: http://apl.aip.org/resource/1/APPLAB/v102/i19
Published by the AIP Publishing LLC.

Tailoring palladium nanocontacts by electromigration

Libe Arzubiaga,[1] Federico Golmar,[1,2] Roger Llopis,[1] Fèlix Casanova,[1,3] and Luis E. Hueso[1,3]
[1]*CIC nanoGUNE Consolider, Tolosa Hiribidea 76, 20018 Donostia—San Sebastian, Basque Country, Spain*
[2]*I.N.T.I.—CONICET, Av. Gral. Paz 5445, Ed. 42, B1650JKA, San Martín, Bs As, Argentina*
[3]*IKERBASQUE, Basque Foundation for Science, 48011 Bilbao, Basque Country, Spain*

(Received 4 February 2013; accepted 26 April 2013; published online 13 May 2013)

Electromigration is employed in nanoelectronics for transforming narrow metallic wires into electrodes separated by a few nanometers gap. In this work, we fabricate either nanoconstrictions or nanogap electrodes by performing electromigration in palladium nanowires. The device resistance and the cross section of the initial nanowires allow us to regulate the conditions for transforming deterministically each nanowire in a specific final device. The resulting samples show unique electrical transport characteristics and could be used in multiple nanoelectronics research applications, from ballistic transport to electrodes for single molecular devices. © *2013 AIP Publishing LLC*. [http://dx.doi.org/10.1063/1.4804559]

Contacting a nano-object (e.g., a nanoparticle, a molecule, or a nanotube) to suitable metallic electrodes is a necessary prerequisite for studying its electronic transport properties.[1–4] Such metallic contacts can be patterned by well-established nanofabrication techniques such as electron-beam lithography or ion-beam-induced deposition. However, most of these conventional techniques are inadequate when the minimum required distance between the electrodes is of the order of 1 nm, which is always the case in the field of single molecular electronics.[5–8]

Among the various alternatives to lithographic techniques, electromigration is widely used for fabricating electrodes of molecular dimensions.[9–12] Electromigration consists on circulating an electric current through a metallic wire of nanometric cross-section until the current density is high enough to cause the migration of metal atoms. This movement of atoms is driven by the energy and momentum transferred by the constant collisions with the incoming electrons. This process causes the failure of the metallic wire by electric fatigue of the material, resulting in the formation of a nanometric gap between closely separated electrodes. Both the shape and the size of the nanometric gap depend on variables that are often difficult to control, such as the grain structure of the metal and the exact distribution of the grain boundaries.[13] This intrinsic variability can alter considerably the output characteristics of the resulting devices, such as the ON current or the gate coupling in the case of field-effect transistors.[14] Thus, increasing the reliability for systematically building devices in which metallic nanocontacts are efficiently fabricated is a major requirement for the research in nanoelectronics.

Gold is the metal which has mostly been used in the fabrication of devices by electromigration.[9,11,13,15,16] Few other metals have been studied, palladium among them, which shows non-standard charge transport features in spite of being also a noble metal. For instance, temperature-dependent features in the zero-bias voltage region of bare palladium nanojunctions have been reported, which seem to constitute an intriguing intrinsic property of this metal.[17] Furthermore, palladium becomes ferromagnetic when alloyed with very low percentage of certain magnetic metals,[18] opening the possibility to be used in spintronic research applications.

In this work, we study electromigration in palladium nanowires. We aim at obtaining a systematic control of the electromigration process in order to use this technique for the fabrication of nanostructures with a given morphology and charge-transport properties. Varying the working conditions in which the electromigration process takes place results in the formation of different structures, from nanoconstrictions to nanogaps of several sizes. Distinctive charge-transport signatures act as a fingerprint of the different fabricated structures otherwise invisible to standard electron microscopy.

We fabricated our devices by electron-beam lithography on top of p-type silicon chips covered by 150 nm of thermally grown silicon oxide. The fabrication was done in a single lithography step, using a double layer of polymethyl metacrylate (PMMA) resist, followed by metal deposition and lift-off. Each chip contained seven devices, each of them consisting of a nanowire with a rectangular-planar geometry contacted by a pair of triangle-shaped microscopic electrodes (see Fig. 1). Palladium and gold (both of 99.99% purity) devices were independently fabricated. In the case of palladium, 20 nm of metal were deposited by magnetron sputtering. In the case of gold, 20 nm of metal were thermally evaporated using a 1.2 nm adhesion layer of titanium. All the devices were cleaned with acetone and isopropanol followed by oxygen plasma before electromigration. The approximate dimensions of the as-produced palladium nanowires were 20 nm in thickness, 300 nm in length, and 60 to 120 nm in width, which gave cross-sections ranging from 1200 to 2400 nm^2. The gold nanowires had the same thickness and length as the palladium ones and widths from 80 to 90 nm, giving approximate cross-sections from 1600 to 1800 nm^2.

Electromigration was performed at 4 K in a liquid helium cryostat with 10 mTorr of helium atmosphere by applying increasing voltage ramps while measuring the current across the devices. Electrical characterization together with scanning electron microscopy (SEM) imaging of the devices

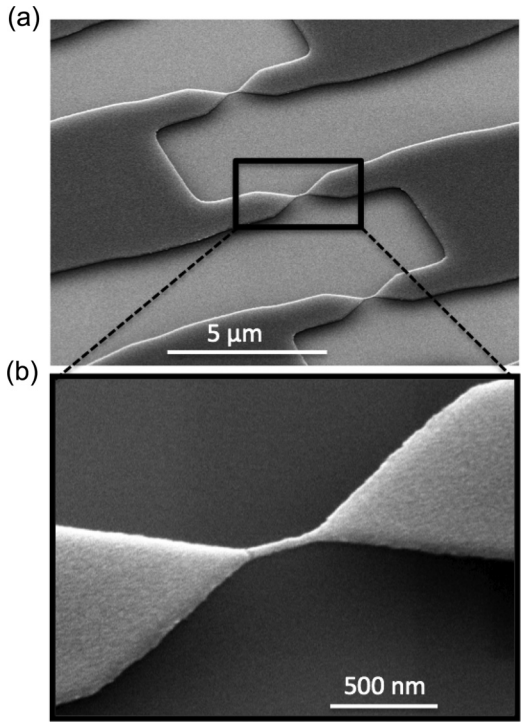

FIG. 1. Scanning electron microscopy image of palladium devices on Si/SiO_2 substrate. (a) Array of several devices on a chip, each consisting on a nanowire contacted by a pair of electrodes (only the microscopic part is shown). (b) Detail of a nanowire contacted with the triangle-shaped ends of the microscopic electrodes.

was performed both before and after the electromigration experiments.

Before the electromigration process took place, the devices showed linear current (I) versus voltage (V) characteristics, as expected. We carried out the electromigration by increasing the voltage across the device at a rate from 3 mV/s to 6 mV/s until the critical current density was reached within the nanowire. At this point, the measured current dropped abruptly, indicating that electromigration had occurred (see Fig. 2). The applied voltage was stopped once the resistance of the device reached a set value.

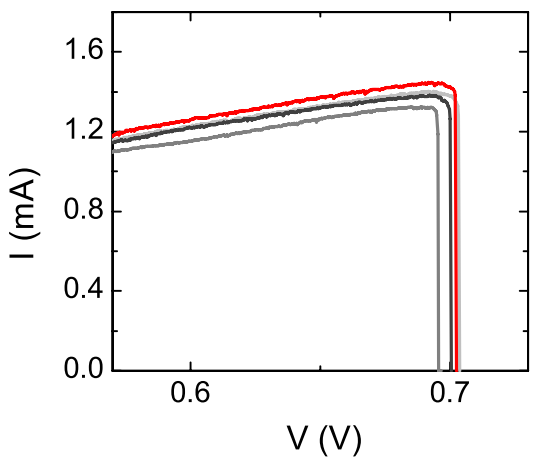

FIG. 2. Current (I)-Voltage (V) curves showing examples of the electromigration process on palladium devices. Four different devices belonging to the same chip are represented, showing the reproducibility of the process. In all four cases, the current increases linearly with the applied voltage, until the critical values (V_C, I_C) are reached and the current drops abruptly.

Electromigration is triggered when a critical current density (J_C) is reached within the nanowires. The current density is related to the critical current (I_C) via the nanowire cross-section (A) ($J_C = I_C / A$). At the same time, I_C and the total resistance of the device (R_{TOTAL}) determine the critical voltage (V_C) at which electromigration takes place ($V_C = I_C \times R_{TOTAL}$). Additionally, R_{TOTAL} is a series sum of the nanowire resistance (R_{NW}) and the resistance of the microscopic and macroscopic contacts (R_{CONT}) conforming the device ($R_{TOTAL} = R_{NW} + R_{CONT}$). The value of R_{TOTAL} (initially, R_0) changes during the electromigration process.

It has been proved experimentally that the critical current and voltage conditions at which electromigration takes place are strongly related to the size and morphology of the obtained gaps.[19,20] We performed a series of electromigration experiments in which the critical voltage value (V_C) at the onset of electromigration was varied. Once the value of the I_C is known for a certain device (uniquely determined by the nanowire cross-section and assuming negligible variations for devices in the same chip, produced in the same fabrication conditions), it is possible to tune V_C by changing the total resistance of the devices.[20,21] This was done by changing the design for the macroscopic part of the devices (using contacts of different length and width) and thus modifying the resistance in series with the nanowires (R_{CONT}). We obtained devices with different total initial resistance (R_0) values by varying the design of the contacts. In Fig. 3, we show V_C and I_C measured at the onset of electromigration of palladium nanowires in 75 different devices. These data have been divided into several intervals according to R_0 value of the devices and represented with a different code (see graph legend).

Through further analysis, we observe that the experimental data (Fig. 3) tend to form two separate groups as a function of R_0. This fact confirms that we can control the onset of electromigration by changing the total resistance. In addition, the data indicate the possible existence of a threshold R_0 value approximately between 0.7 and 1 kΩ separating two different behaviors during electromigration. As observed in Fig. 3, for devices with $R_0 > 1$ kΩ, the onset of electromigration takes place at $V_C > 1.5$ V. Meanwhile, the electromigration for

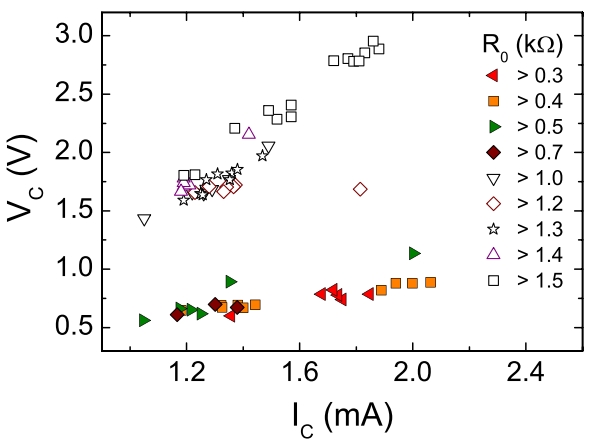

FIG. 3. Critical voltage and current values (V_C, I_C) measured at the onset of electromigration of palladium nanowires in 75 devices. The graph shows two distinct groups of data. The initial total resistance values of the devices in kΩ (R_0) are represented with a different code.

devices with $R_0 < 0.7$ kΩ starts approximately at values of V_C between 0.5 and 0.8 V.

Figure 4 shows the critical voltage as a function of the device resistance at the onset of electromigration (R_C). The cross-sections of the corresponding nanowires have also been represented with a color code in the same graph. The cross-sections were measured from electron microscopy images of the nanowires and x-ray reflectivity measurements of the thickness of thin palladium films deposited simultaneously with the nanowires. We observe that nanowires with a similar cross-section fall in straight lines with slope equal to the average I_C (Fig. 4). Table I displays the average values of J_C calculated according to the I_C extracted from the linear fittings to the data in Fig. 4 and their corresponding range of nanowire cross-section. The average critical current density value (J_C) we obtain from the values in Table I is $(8.8 \pm 0.4) \times 10^{11}$ A/m^2. We observe that J_C is approximately constant for palladium nanowires with the range of cross-sections studied in our experiments (roughly between 1200 and 2400 nm^2). According to literature, J_C can be considered to be constant when performing electromigration in gold nanowires wider than about 60 nm.[13] After our observations, we conclude that palladium also follows this trend.

It must be noted that data regarding electromigration in palladium are scarce in literature, whereas we can find several references to electromigration in gold nanowires reported by different authors.[9–13,15,16,19–26] In order to cross-check our results with the current literature, we have also performed electromigration in 44 gold nanowires. As observed in Fig. 5, the critical current values at the onset of electromigration are centered between 7 and 8.5 mA in our gold devices, which corresponds to a critical current density (J_C) of around 4×10^{12} A/m^2 according to our nanowire dimensions. This value is in good agreement with the ones reported by other authors.[9–13,15,16,19–26] It should be noted that the initial resistance values are lower than those measured for similar palladium devices, due to the lower electrical resistivity of gold with respect to palladium.

The graphs in Fig. 6 show current versus voltage curves for two different palladium devices after electromigration,

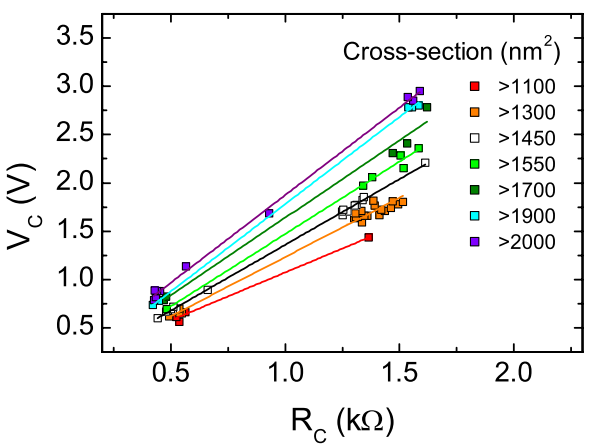

FIG. 4. Critical voltage (V_C) versus total device resistance values at the onset of electromigration (R_C) corresponding to the palladium devices shown in Fig. 3. The color code represents different intervals in the cross-section of the corresponding nanowires. The data corresponding to nanowires with a similar cross-section fall in a straight line of slope equal to I_C.

TABLE I. Experimental values of the average critical current density (J_C) of palladium nanowires and their corresponding range of nanowire cross-section extracted from Fig. 4.

Nanowire cross-section range (nm^2)	J_C (A/m^2)
>1100	8.0×10^{11}
>1300	9.0×10^{11}
>1450	9.1×10^{11}
>1550	9.2×10^{11}
>1700	8.8×10^{11}
>1900	9.2×10^{11}
>2000	8.6×10^{11}

each of them corresponding to one of the distinct groups of data observed in Fig. 3. The device corresponding to Fig. 6(a) is a significant example from the group with $R_0 > 1$ kΩ, whereas the one corresponding to Fig. 6(b) is an example of the group with $R_0 < 0.7$ kΩ. The resulting devices show two very different charge-transport regimes since they have a low bias resistance of about 100 kΩ (Fig. 6(a)) and 10 GΩ (Fig. 6(b)), respectively. The current versus voltage plot for the low resistance devices shows distinct steps, more clearly observed as peaks in the corresponding differential conductance plot (Fig. 6(a)). Instead, the graph in Fig. 6(b) shows a featureless non-linear I versus V curve that fits with the characteristics of a tunneling barrier. We obtain a value of 1.6 ± 0.3 nm for the inter electrode gap size and 1.4 ± 0.5 V for the tunneling barrier height from the fitting to the Simmons equation,[27] using a tunneling effective mass of the free electron and the dielectric constant of vacuum.

In view of these results, we believe that the devices with a final resistance in the kΩ range (Fig. 6(a)) correspond to metallic nanoconstrictions or few-atom contacts. A very rough estimate of the final constriction diameter using the Sharvin resistance formula, and taking into account the device resistance and the electron mean free path in Pd, leads to a result of the order of 1 nm.[28] However, a full characterization by, for example point contact spectroscopy,[29] would be needed for an unambiguous determination of the metallic nature of the devices. Meanwhile, the devices with resistance in the GΩ range, such as the one exemplified in Fig. 6(b),

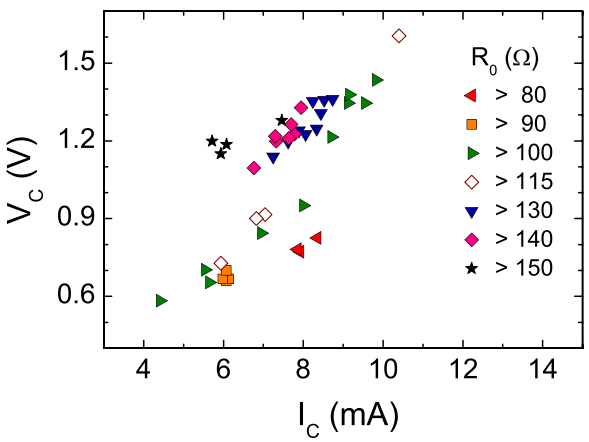

FIG. 5. Critical voltage and current values (V_C, I_C) measured at the onset of electromigration of gold nanowires in 44 devices. The initial total resistance values (R_0) of the devices in Ω are represented with a different code.

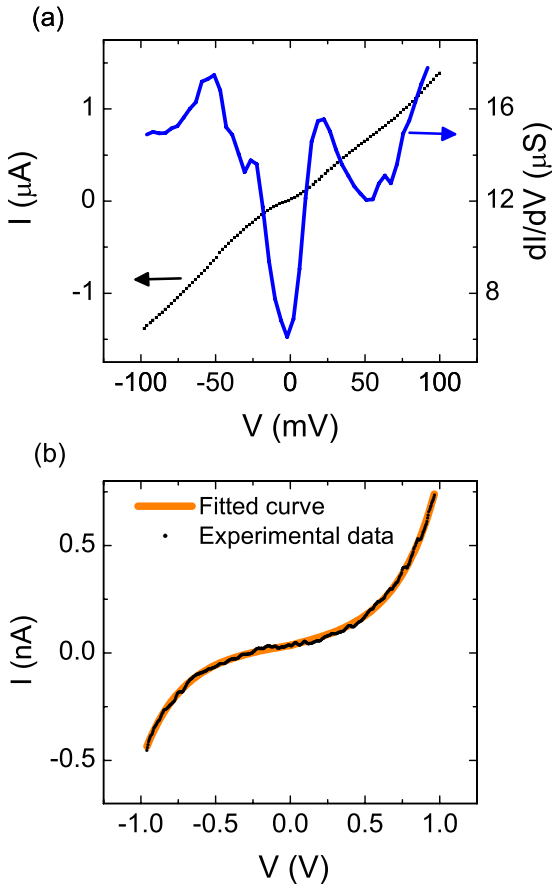

FIG. 6. Electrical characterization of two palladium devices after electromigration. (a) Current (I)-voltage (V) curve of a device with a final resistance of 100 kΩ showing characteristic steps of a metallic nanoconstriction. These features are more easily observed as peaks in the corresponding differential conductance curve. (b) I-V curve of a device with a final resistance of 10 GΩ with a typical shape of a tunneling junction. The fitted curve was calculated using the Simmons equation for tunneling current across an insulating barrier.

show a tunneling charge-transport regime characteristic of electrodes with a gap size between 1 and 2 nm.

In conclusion, we have performed a systematic study of electromigration in palladium nanowires using different working conditions for tailoring the charge-transport characteristics of the obtained devices. The critical current and voltage values at the onset of electromigration can be controlled by changing the cross-section of the nanowires and the total resistance of the system, respectively. Moreover, we have found the existence of a threshold value in the initial resistance, which separates two different sets of resulting devices. Taking advantage of this particular feature, we can control the transformation of our nanowires into either metal nanoconstrictions or electrodes with tunneling nanogaps by carefully choosing the initial device resistance. We have found a strategy for obtaining predictable results when performing electromigration in palladium nanowires and we can employ it for the fabrication of nanodevices of several kinds. However, we must note that the outcome of electromigration depends strongly on the nature of the metal. It is, therefore, necessary to study carefully each case in order to find the adequate experimental conditions for a systematic fabrication of devices.

This work was supported by the European Union 7th Framework Programme under the Marie Curie Actions (PIRG06-GA-2009-256470), the European Research Council (Grant 257654-SPINTROS), the Spanish Ministry of Science and Education under Project No. MAT2009-08494, as well as by the Basque Government through Project No. PI2011-1. L.A. thanks the Basque Government for a Ph.D. fellowship (BFI09.160).

[1]D. L. Klein, R. Roth, A. K. L. Lim, A. P. Alivisatos, and P. L. McEuen, Nature **389**, 699 (1997).
[2]S. Kubatkin, A. Danilov, M. Hjort, J. Cornil, J. L. Brédas, N. Stuhr-Hansen, P. Hedegård, and T. Bjørnholm, Nature **425**, 698 (2003).
[3]A. S. Blum, J. G. Kushmerick, D. P. Long, C. H. Patterson, J. C. Yang, J. C. Henderson, Y. Yao, J. M. Tour, R. Shashidhar, and B. R. Ratna, Nature Mater. **4**, 167 (2005).
[4]J. F. Dayen, V. Faramarzi, M. Pauly, N. T. Kemp, M. Barbero, B. P. Pichon, H. Majjad, S. Begin-Colin, and B. Doudin, Nanotechnology **21**, 335303 (2010).
[5]F. Chen, Q. Qing, L. Ren, Z. Wu, and Z. Liu, Appl. Phys. Lett. **86**, 123105 (2005).
[6]S. M. Luber, F. Zhang, S. Lingitz, A. G. Hansen, F. Scheliga, E. Thorn-Csányi, M. Bichler, and M. Tornow, Small **3**, 285 (2007).
[7]M. Ruben, A. Landa, E. Lörtscher, H. Riel, M. Mayor, H. Görls, H. B. Weber, A. Arnold, and F. Evers, Small **4**(12), 2229 (2008).
[8]J. Fursina, S. Lee, R. G. S. Sofin, I. V. Shvets, and D. Natelson, Appl. Phys. Lett. **92**, 113102 (2008).
[9]H. Park, A. K. L. Lim, A. P. Alivisatos, J. Park, and P. L. McEuen, Appl. Phys. Lett. **75**, 301 (1999).
[10]J. Park, A. N. Pasupathy, J. I. Goldsmith, C. Chang, Y. Yaish, J. R. Petta, M. Rinkoski, J. P. Sethna, H. D. Abruña, P. L. McEwen, and D. C. Ralph, Nature **417**, 722 (2002).
[11]A. K. Mahapatro, J. Ying, T. Ren, and D. B. Janes, Nano Lett. **6**, 123 (2006).
[12]H. Song, Y. Kim, Y. H. Jang, H. Jeong, M. A. Reed, and T. Lee, Nature **462**, 1039 (2009).
[13]C. Durkan, M. A. Schneider, and M. E. Welland, J. Appl. Phys. **86**, 1280 (1999).
[14]E. A. Osorio, T. Bjørnholm, J. M. Lehn, M. Ruben, and H. S. J. van der Zant, J. Phys.: Condens. Matter **20**, 374121 (2008).
[15]D. R. Strachan, D. E. Smith, D. E. Johnston, T. H. Park, M. J. Therien, D. A. Bonnell, and A. T. Johnson, Appl. Phys. Lett. **86**, 043109 (2005).
[16]R. Vincent, S. Klyatskaya, M. Ruben, W. Wernsdorfer, and F. Balestro, Nature **488**, 357 (2012).
[17]G. D. Scott, J. J. Palacios, and D. Natelson, ACS Nano **4**, 2831 (2010).
[18]S. Hornfeldt, J. B. Ketterson, and L. R. Windmiller, Phys. Rev. Lett. **23**, 1292 (1969).
[19]M. L. Trouwborst, S. J. van der Molen, and B. J. van Wees, J. Appl. Phys. **99**, 114316 (2006).
[20]J. J. Henderson, C. M. Ramsey, and E. del Barco, J. Appl. Phys. **101**, 09E102 (2007).
[21]C. B. Winkelmann, N. Roch, W. Wernsdorfer, V. Bouchiat, and F. Balestro, Nat. Phys. **5**, 876 (2009).
[22]D. Demarchi, P. Civera, G. Piccinini, M. Cocuzza, D. Perrone, Electrochim. Acta **54**, 6003 (2009).
[23]A. N. Pasupathy, R. C. Bialczak, J. Martinek, J. E. Grose, L. A. K. Donev, P. L. McEuen, and D. C. Ralph, Science **306**, 86 (2004).
[24]R. Sordan, K. Balasubramanian, M. Bughard, and K. Kern, Appl. Phys. Lett. **87**, 013106 (2005).
[25]A. N. Pasupathy, J. Park, C. Chang, A. V. Soldatov, S. Lebedkin, R. C. Bialczak, J. E. Grose, L. A. K. Donev, J. P. Sethna, D. C. Ralph, and P. L. McEuen, Nano Lett. **5**, 203 (2005).
[26]N. Roch, S. Florens, V. Bouchiat, W. Wernsdorfer, and F. Balestro, J. Low Temp. Phys. **153**, 358 (2008).
[27]J. G. Simmons, J. Appl. Phys. **34**, 1793 (1963).
[28]Yu. V. Sharvin, Sov. Phys. JETP **21**, 655 (1965).
[29]V. N. Antonov, A. V. Zhalko-Titarenko, V. Yu Milman, A. V. Khotkevich, and S. N. Krainyukov, J. Phys.: Condens. Matter **3**, 6523 (1991).